J. Am. Chem. Soc. 1994, 116, 2821–2826

In Situ Near-Infrared Spectroscopic Investigation of Epoxy Resin–Aromatic Amine Cure Mechanisms

L. Xu, J. H. Fu,[†] and J. R. Schlup[*]

Contribution from the Department of Chemical Engineering, Durland Hall, Kansas State University, Manhattan, Kansas 66506-5102

Received July 8, 1993[⊗]

Abstract: Accurate models of epoxy cure reactions are essential for intelligent processing of polymer matrix composites. In the near-infrared region, the absorption peaks characteristic of the epoxide, secondary amine, and hydroxyl groups are well-isolated from neighboring absorptions. This enables epoxy resin cure reactions to be successfully monitored via *in situ* near-infrared Fourier transform spectroscopy. In order to elucidate the mechanisms involved in the reaction between epoxy resins and amines, various proposed mechanisms, and their corresponding rate equations, are considered herein. A model system comprised of phenyl glycidyl ether and methylaniline was used to obtain conversion rate data. The reaction mechanism was found to be described fully by a two-parameter model. Arrhenius-type temperature dependencies were demonstrated for both rate constants. Activation energies of 16.5 ± 1.4 and 13.1 ± 1.0 kcal/mol were obtained for the uncatalyzed and catalyzed reactions, respectively.

Introduction

Epoxy resins have been studied extensively over the past several decades and, due to their ever expanding application in industry, continue to receive substantial research interest worldwide. The kinetics and mechanisms of the cure reactions have long been the focus of epoxy resin research. Since the commercial debut of epoxy resins in the late 1940's, numerous research papers have been published concerning these reactions. Several excellent review articles on the kinetics and mechanisms of epoxy resin cure reactions are available.[1-5] Unfortunately, most of the work has remained empirical in nature, with conversion data being fit to empirical, power law-type equations. Only a few references have considered the fundamental reaction mechanisms involved in curing epoxy resins.[3,6-10]

Shechter[6] first proposed a "push–pull" mechanism. He suggested that the reaction of an epoxide group with an amine occurs through a termolecular intermediate consisting of an epoxide group, an amine, and a hydroxyl group. This is a concerted displacement mechanism similar to a bimolecular nucleophilic substitution (S$_N$2) reaction. Smith[7] proposed a variation of Shechter's mechanism based on the argument that the termolecular intermediate proposed by Shechter is unlikely to form in one step. Smith suggested that a hydrogen bond forms between the hydroxyl group and the oxirane group of the epoxide. A termolecular transition state, identical with the one proposed by Shechter, then forms by the addition of the amine to the complex. Tanaka and Mika[8] suggested another mechanism based on the formation of a hydrogen bond between an amine and a hydroxyl group. They argued that hydrogen bonding between hydroxyl and amine groups would be more favorable than that between hydroxyl and oxirane groups due to the differences in their basicities. Rozenberg[3] reviewed the possibilities of reactions between epoxy groups and amines in the absence of the hydroxyl groups. He concluded that the amine will be bifunctional, acting both as a nucleophilic and an electrophilic reagent when hydroxyl groups are absent. Two different mechanisms were proposed corresponding to those suggested by Smith[7] and by Tanaka and Mika,[8] except that the hydroxyl groups were replaced by amine groups.

Investigations into the mechanisms for epoxide resin cure reactions continue, but experimental evidence obtained to date has apparently not been sufficient to unambiguously discriminate between various proposed mechanisms. Although research efforts constantly attempt to verify proposed mechanisms, including a recent investigation conducted by Mijovic and co-workers,[10] the problem has remained unsolved.

Kinetic models for the epoxy resin cure have been developed in one of two ways. One approach relies on simple *n*th-order kinetics[11-15] while the other involves modeling autocatalytic reaction mechanisms.[16-22] While these kinetic studies are valuable for process design, neither approach has been based on the fundamental reaction mechanisms. In addition, the application of empirical or semiempirical kinetics must be confined to those conditions used to establish the kinetic relationships.

Fourier transform infrared (FTIR) spectroscopy is an important tool in monitoring the cure reactions of epoxy resins with hardeners. In such studies, the mid-infrared region of the spectrum typically is utilized since the functional groups involved

---

[†] Department of Basic Courses, Luoyang Institute of Technology, Luoyang, Henan 471039, PRC.

[*] Author to whom correspondence should be addressed.

[⊗] Abstract published in *Advance ACS Abstracts,* March 1, 1994.

(1) Barton, J. M. *Adv. Polym. Sci.* **1985**, *72*, 111–154.

(2) Dusek, K. *Adv. Polym. Sci.* **1985**, *78*, 1–50.

(3) Rozenberg, B. A. *Adv. Polym. Sci.* **1985**, *75*, 113–165.

(4) Oleinik, E. F. *Adv. Polym. Sci.* **1985**, *80*, 50–99.

(5) Tanaka, Y.; Bauer, R. S. In *Epoxy Resins Chemistry and Technology*, 2nd ed.; May, C. A., Ed.; Marcel Dekker: New York, 1988; pp 285–463.

(6) Schechter, L.; Wynstra, J.; Kurkjy, R. P. *Ind. Eng. Chem.* **1956**, *48*, 94–97.

(7) Smith, I. R. *Polymer* **1961**, *2*, 95–108.

(8) Tanaka, Y.; Mika T. F. In *Epoxy Resins Chemistry and Technology*, May, C. A., Tanaka, Y., Eds.; Marcel Dekker: New York, 1973, pp 135–239.

(9) King, J. J.; Bell J. P. In *Epoxy Resin Chemistry*; Bauer R. S., Ed.; ACS Symp. No. 114; American Chemical Society: Washington, DC, 1979; pp 225–257.

(10) Mijovic, J.; Fishbain, A.; Vijova, J. *Macromolecules* **1992**, *25*, 979–985.

(11) Acitelli, M. A.; Prime, R. B.; Sacher, E. *Polymer* **1971**, *12*, 335–343.

(12) Prime, R. B. In *Analytical Calorimetry*; Porter, R. S., Johnson, J. F., Eds.; Plenum Press: New York, 1970; Vol. 2, pp 201–210.

(13) Prime, R. B. *Polym. Eng. Sci.* **1973**, *13(1)*, 365–371.

(14) Prime, R. B.; Sacher, E. *Polymer* **1972**, *13*, 455–458.

(15) Barton, J. M. *Makromol. Chem.* **1973**, *171*, 247–251.

(16) Horie, K.; Hiura, H.; Sawada, M.; Mita, I.; Kambe, H. *J. Polym. Sci.* **1970**, *8*, 1357–1372.

(17) Kamal, M. R.; Sourour, S.; Ryan, M. *Soc. Plast. Eng. Tech. Papers* **1973**, *19*, 187.

(18) Sourour, S.; Kamal, M. R. *Thermochim. Acta* **1976**, *14*, 41–59.

(19) Ryan, M. E.; Datta, A. *Polymer* **1979**, *20*, 203–206.

(20) Flammersheim, H. J.; Hörhold, H. H.; Bellstedt, K.; Klee, J. *Makromol. Chem.* **1983**, *184*, 113–121.

(21) Spacek, V.; Pouchly, J.; Biros, J. *Eur. Polym. J.* **1987**, *23(5)*, 377–382.

(22) Chiao, L.; Lyon, R. *J. Composite Mater.* **1990**, *24*, 739–752.

0002-7863/94/1516-2821$04.50/0

in epoxy resin cure reactions all have strong characteristic absorptions in the mid-infrared region. However, the MIR spectra of epoxy resins and hardeners are very complex. Well-isolated primary amine, secondary amine, and hydroxyl group absorption bands often are not observed, which leads to complications in obtaining quantitative analysis via infrared spectroscopy.[23] The functional groups of interest in epoxy resin cure reactions typically have well-isolated absorption bands in the near-infrared (NIR) region of the spectrum (10000 to 4000 cm^{-1}). This is a consequence of the absorption bands in the NIR resulting from overtone and combination bands. NIR spectroscopy presents several potential advantages over MIR spectroscopy for characterizing the cure reactions of epoxy resin systems, such as enhanced resolution, higher energy sources, and lower oscillator strengths.[24,25]

Characterization of epoxy resin cure reactions by NIR spectroscopy began in the late 1950's. Goddu and Delker[26] identified two characteristic bands in the NIR region (at 6061 and 4546 cm^{-1}) for the terminal epoxide group and discussed band interferences between epoxide bands and C–H absorptions. Dannenberg[27] utilized NIR spectroscopy to investigate epoxy–amine cure reactions. Both epoxide and hydroxyl group absorptions were quantified, and the effects of hydrogen bond formation on the spectra obtained were addressed. Schiering and Katon[28] studied the reaction between diglycidyl ether of bisphenol A (DGEBA) and metaphenylenediamine. Both MIR and NIR spectra were used to quantify the terminal epoxide bands as well as amine and hydroxyl groups. The absorption at 914 cm^{-1} in the MIR spectra was chosen for analysis of the epoxide group. Data for primary amine, secondary amine, and hydroxyl group concentrations were obtained from NIR spectra. Paputa Peck and co-workers[29] quantified the cure of epoxy coating systems using NIR spectroscopy. Epoxy ring concentrations could be determined during synthesis and cross-linking utilizing the terminal epoxide group NIR absorption at 4532 cm^{-1}. More recently, Miller[30] has reviewed the application of NIR spectroscopy in studies of synthetic polymers, including epoxy resin cure reactions.

The applicability of NIR spectroscopy for studying the epoxide resin cure mechanisms and their chemical kinetics is demonstrated herein. Specifically, kinetic data for the reactions of phenyl glycidyl ether (PGE) with methylaniline (mAnil) are presented. Fundamental reaction mechanisms are explored. This system is ideal for developing *in situ* FTIR techniques to study epoxy cure reactions for several reasons. The PGE/mAnil system itself is a liquid solution; thus, interferences from solvents can be avoided. While the reactions which occur between PGE and mAnil are typical of epoxy cure reactions, both reactants are monofunctional. Since polymerization does not occur, interpretation of the data is greatly simplified. The formation of a simple product significantly limits the complexity of the rate expressions. In addition, the epoxide, hydroxyl, and amine groups can be observed unambiguously. The advantages of NIR spectroscopy permit unique perspectives to be obtained; in particular, reaction rate data can be acquired *in situ* and with sufficient quality to allow differential analysis of the data.

Table 1. Peak Assignments for the NIR Spectra

band	peak position, cm^{-1}	integration range, cm^{-1}
epoxide combination	4526	4502–4551
secondary amine overtone	6660	6603–6771
hydroxyl group overtone	7000	6901–7100
aromatic ring C–H stretch combination	5969	5932–6049

Experimental Section

Phenyl glycidyl ether (1,2-epoxy-3-phenoxypropane (PGE), Aldrich Chemical Co., 99% purity) and *N*-methylaniline (mAnil, Aldrich Chemical Co., 99+% purity) were the epoxide and curing agent studied. Both reagents were used as received.

The near-infrared spectroscopic data were acquired with a SpectraTech high-temperature transmission cell in a Mattson Nova Cygni 120 FTIR spectrometer. A tungsten halogen source was used along with a quartz beamsplitter and an indium antimonide detector. The windows for the transmission cell were sodium chloride disks with a 0.5-mm lead spacer between the windows. At each time interval, 16 spectra at 8-cm^{-1} resolution were co-added.

The uncured mixture having stoichiometric quantities of amine and epoxide was placed in the high-temperature transmission sample cell at room temperature. One spectrum was obtained prior to heating the sample cell. The cell then was heated and NIR spectra of the reacting mixture were obtained *in situ* as a function of time. The system can be treated as a differential batch reactor due to the small volume of the sample.

The concentrations of epoxide, secondary amine, and hydroxyl groups were characterized from the integrated intensity of the epoxide combination band at 4526 cm^{-1}, the secondary amine overtone band at 6660 cm^{-1}, and the hydroxyl group overtone band at 7000 cm^{-1}, respectively. All absorptions were normalized against the aromatic ring C–H stretch combination band at 5969 cm^{-1}, thus providing an internal standard. The integrated intensities were used throughout the analysis (see Table 1). In particular, a slice-area technique was used. Details on band assignments have been discussed elsewhere.[23]

Model Development

It is generally agreed that during cure of epoxy resins with amines the following reactions take place:

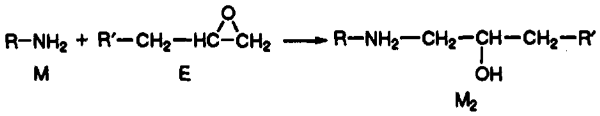

$$\mathrm{R{-}NH_2} + \mathrm{R'{-}CH_2{-}\overset{O}{HC{-}CH_2}} \longrightarrow \mathrm{R{-}NH_2{-}CH_2{-}\underset{OH}{CH}{-}CH_2{-}R'} \quad \text{(I)}$$

$$\underset{\mathrm{M}}{} \qquad \underset{\mathrm{E}}{} \qquad \underset{\mathrm{M_2}}{}$$

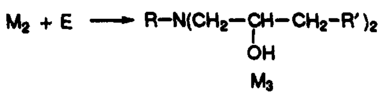

$$\mathrm{M_2} + \mathrm{E} \longrightarrow \underset{\mathrm{M_3}}{\mathrm{R{-}N(CH_2{-}\underset{OH}{CH}{-}CH_2{-}R')_2}} \quad \text{(II)}$$

Other possible reactions include homopolymerization of epoxy resins and etherification between neighboring epoxy oxirane and hydroxyl groups. However, homopolymerization of epoxy resin will only occur in the presence of Lewis bases, inorganic bases, or Lewis acid catalysts.[6,31] For certain epoxy resin–amine systems, etherification may occur; but, the reaction rate will be significant only at high temperatures and at high degrees of cure. Therefore, it is reasonable to neglect both the homopolymerization and etherification in the analysis of the data described herein.

Previously proposed models for epoxy cure reactions can be classified into three types (Scheme 1). Type A includes formation of hydrogen-bonded epoxy species as the initial step, followed by the formation of a termolecular intermediate involving epoxy, amine, and HX (either hydroxyl or amine) functional groups. Type B involves the formation of hydrogen-bonded amine as the initial step, followed by the formation of the same termolecular intermediate as in type A. Type C consists of the simultaneous formation of hydrogen-bonded epoxy and hydrogen-bonded amine as its first step. The formation of an intermediate complex involving hydrogen-bonded epoxy and hydrogen-bonded amine follows. For the PGE/mAnil system, these proposed mechanisms would occur as shown below.

---

[23] Fu, J. H.; Schlup, J. R. *J. Appl. Polym. Sci.* In press.
[24] Whetsel, K. B. *Appl. Spectrosc. Rev.* **1968**, *2*, 1–67.
[25] Stark, E.; Luchter, K.; Margoshes, M. *Appl. Spectrosc. Rev.* **1986**, *22*, 335–399.
[26] Goddu, R. F.; Delker, D. A. *Anal. Chem.* **1958**, *30*, 2013–2016.
[27] Dannenberg, H. *Soc. Plast. Eng. Trans.* **1963**, *3*, 78–88.
[28] Schiering, D. W.; Katon, J. E. *J. Appl. Polym. Sci.* **1987**, *34*, 2367–2375.
[29] Paputa Peck, M. C.; Carter, R. O., III; Qaderi, S. B. A. *J. Appl. Polym Sci.* **1987**, *33*, 77–86.
[30] Miller, C. E. *Appl. Spectrosc. Rev.* **1991**, *26*, 277–399.
[31] Potter, W. G. *Epoxide Resins*; The Plastics Institute, Iliffe Books: London, 1970; pp 48–51.

Scheme 1. Three Previously Proposed Models for Epoxy Cure Reactions

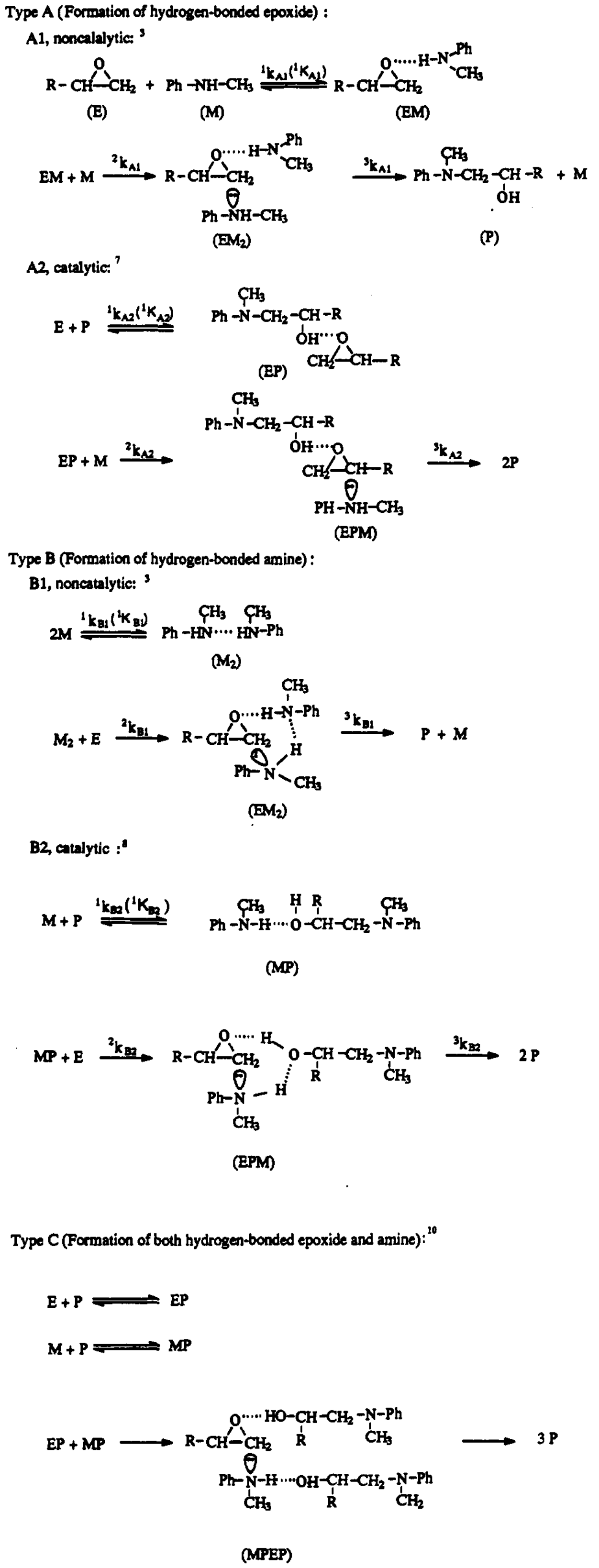

Since hydroxyl groups are believed to be catalysts for the cure reaction, the production of hydroxyl groups as a part of the reaction scheme clearly implies the process is autocatalytic. A1 and B1 are called noncatalytic paths; the others are known as catalytic paths. Obviously, path A1 or B1 will only be important at the early stage of the reaction when the hydroxyl group concentration is low.

While different combinations of noncatalytic and catalytic paths potentially create several mechanisms (*e.g.* A1 + A2 + C, B1 + A2 + C, A1 + B2 + C, B1 + B2 + C, *etc.*), from theoretical considerations it can be seen that some paths are more likely than others. This enables less feasible paths to be eliminated from consideration. In order for the reaction to proceed *via* path B2, the hydrogen-bonded species formed in the first step must takes the form

–N–H···Ö–H

I

However, since the acidity of a hydroxyl group is much higher than that of an amine, the hydrogen bond between the hydroxyl group and the amine will tend to form as

H–N̈···H–O

II

Obviously, by forming structure **II**, the lone pair electrons of the amine nitrogen are already involved in bond formation and the nitrogen loses its ability to attack the α-carbon atom of the epoxide oxirane group. While the real situation may be that both structures **I** and **II** are formed, the amount of structure **II** formed will far exceed that of structure **I**. Therefore, structure **I** can be neglected, and consequently, the reaction most likely proceeds via B1 instead of B2. The same line of reasoning is applicable to path C as well.

Therefore, it is reasonable to assume that the predominant mechanisms for epoxy amine cure are A1 plus A2 or B1 plus A2. Kinetic expressions are derived easily for these mechanisms with the outcome depending upon which step is assumed to be rate determining. Both A1 + A2 and B1 + A2 consist of three reaction steps. The following kinetic equations were obtained with the designated step assumed to be rate determining (RDS):

Case 1: Step 1 as RDS

For A1 + A2

$$-\frac{d[M]}{dt} = {}^1k_{A1}[E][M] + {}^1k_{A2}[E][P] \tag{1}$$

For B1 + A2

$$-\frac{d[M]}{dt} = {}^1k_{B1}[M]^2 + {}^1k_{A2}[E][P] \tag{2}$$

where ${}^1k_{A1}$, ${}^1k_{A2}$, and ${}^1k_{B1}$ are the reaction rate constants of the first step in paths A1, A2, and B1, respectively.

Case 2: Step 2 as RDS

For A1

$$-\frac{d[M]}{dt} = {}^2k_{A1}{}^1K_{A1}[E][M]^2 \tag{3}$$

For A2

$$\frac{d[M]}{dt} = {}^2k_{A2}{}^1K_{A2}[M][E][P] \tag{4}$$

where ${}^2k_{A1}$, ${}^1K_{A1}$, ${}^2k_{A2}$, and ${}^1K_{A2}$ are the reaction rate constants of the second step and the equilibrium constants of the first step in paths A1 and A2, respectively.

For B1

$$[M_2] = {}^1K_{B1}[M]^2 \tag{5}$$

$$\frac{d[M_2]}{dt} = 2{}^1K_{B1}[M]\frac{d[M]}{dt} \tag{6}$$

At the same time

$$\frac{d[M_2]}{dt} = {}^2k_{B1}{}^1K_{B1}[E][M]^2 \qquad (7)$$

From eqs 6 and 7

$$-\frac{d[M]}{dt} = \frac{1}{2}{}^2k_{B1}[E][M] \qquad (8)$$

where ${}^2k_{B1}$ and ${}^1K_{B1}$ are the reaction rate constant of the second step and the equilibrium constant of the first step in path B1.

Therefore, for A1 + A2

$$-\frac{d[M]}{dt} = k'_{A1}[E][M]^2 + k'_{A2}[E][M][P] \qquad (9)$$

where $k'_{A1} = {}^2k_{A1}{}^1K_{A1}$ and $k'_{A2} = {}^2k_{A2}{}^1K_{A2}$.

For B1 + A2

$$-\frac{d[M]}{dt} = \frac{1}{2}{}^2k_{B1}[E][M] + k'_{A2}[E][M][P] \qquad (10)$$

Case 3: Step 3 as RDS

For A1

$$[EM_2] = {}^1K_{A1}{}^2K_{A1}[M]^2 \qquad (11)$$

$$\frac{d[EM_2]}{dt} = {}^1K_{A1}{}^2K_{A1}\left([M]^2\frac{d[E]}{dt} + 2[E][M]\frac{d[M]}{dt}\right) \qquad (12)$$

where ${}^1K_{A1}$ and ${}^2K_{A1}$ are the equilibrium constants for steps 1 and 2, respectively, in path A1. At the same time,

$$\frac{d[EM_2]}{dt} = -{}^3k_{A1}{}^1K_{A1}{}^2K_{A1}[E][M]^2 \qquad (13)$$

where ${}^3k_{A1}$ is the reaction rate constant of step 3 in path A1.

From eqs 12 and 13

$$-\frac{d[M]}{dt} = \frac{1}{2}{}^3k_{A1}[M] + \frac{1}{2}\frac{[M]}{[E]}\frac{d[E]}{dt} \qquad (14)$$

Similarly, for B1

$$-\frac{d[E]}{dt} = \frac{1}{2}{}^3k_{B1}[M] + \frac{1}{2}\frac{[M]}{[E]}\frac{d[E]}{dt} \qquad (15)$$

where ${}^3k_{B1}$ is the reaction rate constant of step 3 in path B1.

For A2

$$-\frac{d[M]}{dt} = {}^3k_{A2}[M] + \frac{[M]}{[P]}\frac{d[P]}{dt} + \frac{[M]}{[E]}\frac{d[E]}{dt} \qquad (16)$$

where ${}^3k_{A2}$ is the reaction rate constant of step 3 in path A2.

Therefore, For A1 + A2

$$-\frac{d[M]}{dt} = \left(\frac{1}{2}{}^3k_{A1} + {}^3k_{A2}\right)[M] + \frac{[M]}{[P]}\frac{d[P]}{dt} + \frac{3}{2}\frac{[M]}{[E]}\frac{d[E]}{dt} \qquad (17A)$$

For B1 + A2

$$-\frac{d[M]}{dt} = \left(\frac{1}{2}{}^3k_{B1} + {}^3k_{A2}\right)[M] + \frac{[M]}{[P]}\frac{d[P]}{dt} + \frac{3}{2}\frac{[M]}{[E]}\frac{d[E]}{dt} \qquad (17B)$$

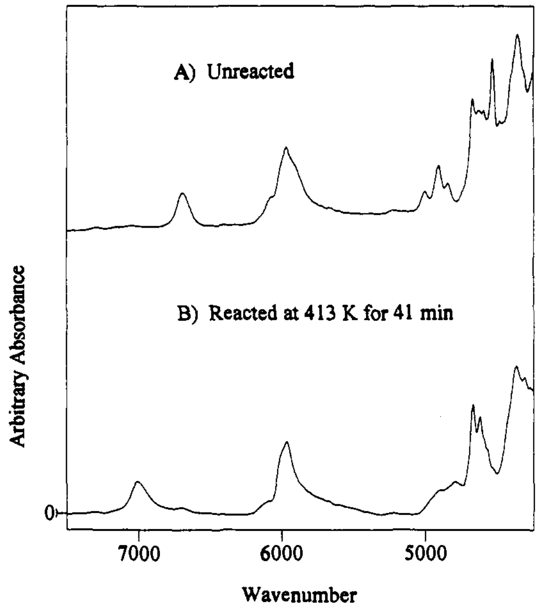

Figure 1. NIR spectra of PGE/mAnil. (A) unreacted; (B) following reaction at 413 K for 41 min.

Mijovic and co-workers[10] performed similar analyses for the kinetics of epoxy–amine cure reactions. However, in order to successfully describe the experimental data, they had to introduce empirical parameters described as weight factors, *w*. Since the determination of the weight factors is rather arbitrary, the application of their reaction model is greatly limited. By excluding reaction path C which, as pointed out earlier, is not supported by theoretical justifications, the kinetic equations derived are much simpler and, most importantly, the use of additional empirical parameters in the kinetic equations can be avoided.

Results and Discussion

The NIR infrared spectra of PGE/mAnil, both unreacted and reacted (at 413 K for 41 min), are shown in Figure 1. It is seen from the figure that absorption peaks characteristic of the secondary amine and hydroxyl groups (at 6660 and 7000 cm^{-1}, respectively) are well-isolated from neighboring absorptions. While a broad absorption is present in the baseline beneath the epoxide absorption at 4526 cm^{-1}, the epoxide peak is isolated above this baseline and yields integrated absorption data suitable for quantitative analysis. Therefore, quantitative analysis of the experimental data can be performed with good accuracy.

In situ NIR monitoring of an epoxy–amine cure reaction at isothermal (413 K) conditions is demonstrated in a three-dimensional plot (Figure 2). Figure 3 shows the kinetic data obtained from Figure 2 for the disappearance of epoxide and secondary amine functional groups with the subsequent generation of hydroxyl groups. All data are expressed in terms of the absorption ratios described earlier. The autocatalytic nature of epoxy–amine cure is evident from the S-shaped character of the curve. Since absorbance is directly proportional to the concentration according to Beer's law, the experimental data shown in Figure 3 and the rate equations derived in the previous section were used directly to quantitatively describe the conversion data.

In Figure 4 the experimental conversion rate data were compared with predicted values obtained by fitting the model derived for mechanism A1 + A2. It is obvious from Figure 4 that, if the formation of the termolecular complex (step 2) is assumed to be the rate-determining step (Case 2), the model provides an excellent fit to the experimental data over the entire time during which the reaction was monitored. The appropriate reaction rate constants were obtained from least-squares linear regression analysis. Case 3, assuming the decomposition of the

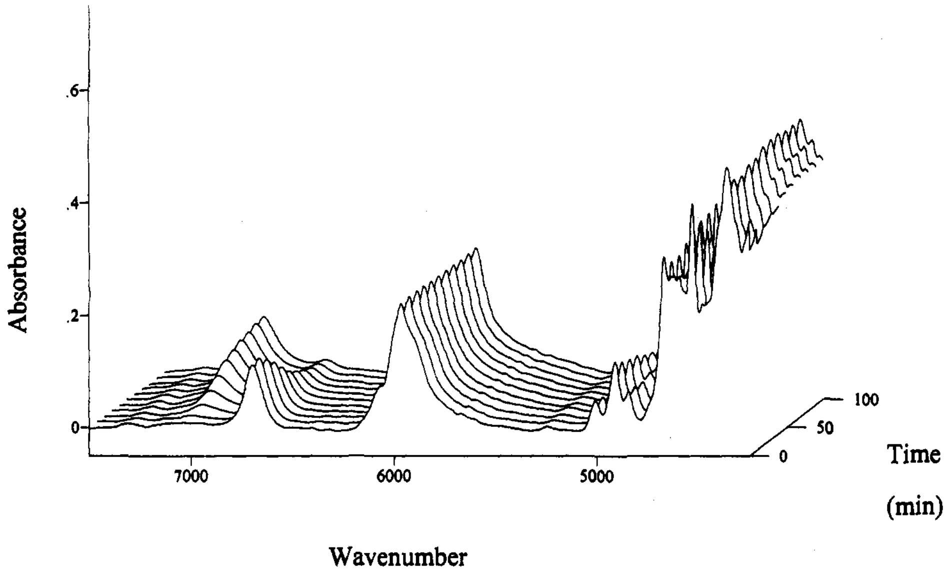

Figure 2. *In situ* absorption spectra for the PGE/mAnil reaction at 413 K.

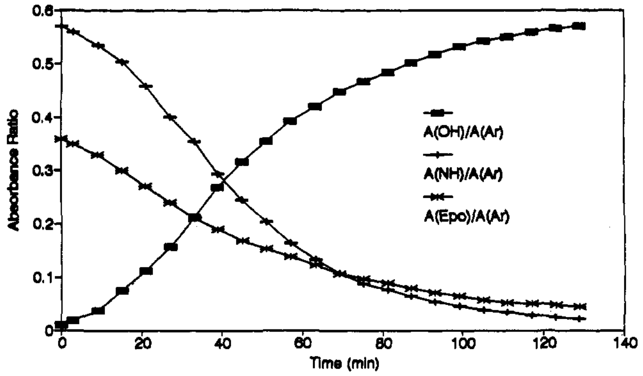

Figure 3. Absorbance ratio *vs* time for the PGE/mAnil reaction at 413 K.

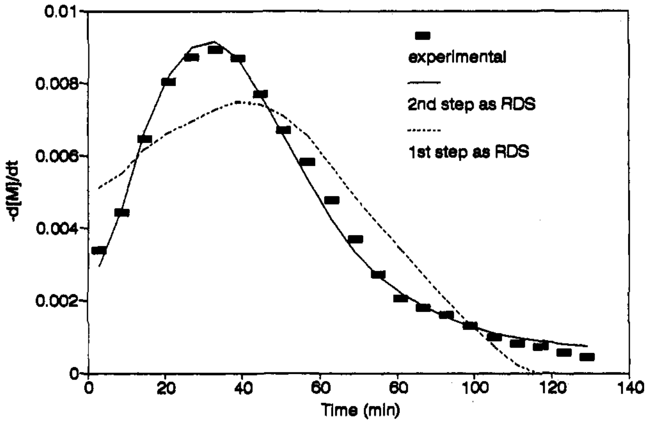

Figure 4. Comparison of experimental and predicted conversion data for mechanism A1 + A2.

termolecular complex (step 3) as the rate-determining step, was not included in the figure since it leads to reaction rate constants less than zero. This is not physically possible; thus, these reactions were eliminated from consideration. Therefore, it is quite clear that the reaction follows mechanisms A1 + A2 or B1 + A2 with the second step in the reaction sequence being the rate-determining step.

From the available experimental data, it is still not possible to distinguish between paths A1 and B1. The reaction rate constant for path A1 or B1 is more than one order of magnitude smaller than the one for path A2. In other words, path A1 or B1 will only be significant at the early stage of the reaction when hydroxyl concentration is relatively low. Therefore, it will be difficult to distinguish between these two reaction paths with the possible exception of the earliest reaction stages in a highly purified system.

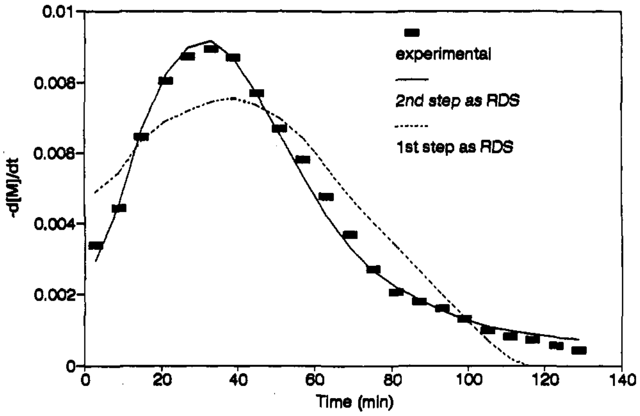

Figure 5. Comparison of experimental and predicted conversion data for mechanism B1 + A2.

The above analysis was based on absorption ratios rather than absolute concentrations. In order for the reaction rate constants to be determined with their proper units, the rate equations need to be rewritten in terms of conversion of the reaction. Dividing eqs 9 and 10 by $[E_0]^2$ where ($[E_0]$ = initial concentration of epoxide), the expressions below are obtained.

For mechanism A1 + A2

$$\frac{d[\alpha]}{dt} = [E_0]^2[k'_{A1}(1-\alpha) + k'_{A2}\alpha](1-\alpha)^2 \qquad (18)$$

For mechanism B1 + A2

$$\frac{d\alpha}{dt} = [E_0][{}^2k_{B1} + [E_0]k'_{A2}\alpha](1-\alpha)^2 \qquad (19)$$

where α is the conversion of the reaction and is equal to $(1 - [E]/[E_0])$.

$[E_0]$ can be calculated based upon the stoichiometry of the reaction. For equimolar addition of PGE and mAnil, $[E_0]$ = 4.11 mol/L. According to the Beer's law, the absorbance A of a component i is proportional to its concentration [i]. $[E]/[E_0]$ is equal to A_E/A_{E0}; the later is easily obtained from the experimental data described herein. The time dependence of the

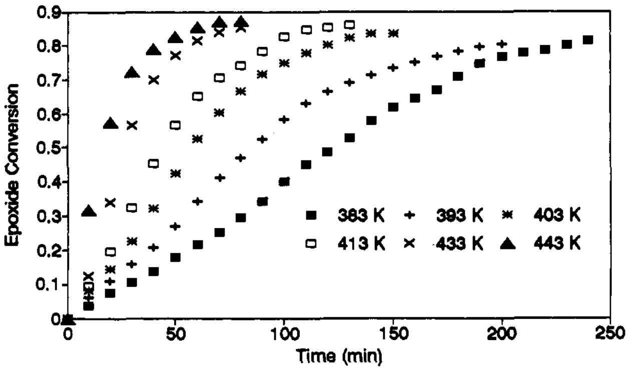

Figure 6. Time dependence of the conversion for the PGE/mAnil reaction.

conversion α is shown in Figure 6 for different reaction temperatures ranging from 383 to 443 K.

Values for k'_{A1}, ${}^2k_{B1}$, and k'_{A2} were determined at different reaction temperatures based upon fitting the conversion data to eqs 18 and 19. Arrhenius-type relationships were demonstrated for k'_{A1}, ${}^2k_{B1}$, and k'_{A2} (Figure 7). Activation energies as well as pre-exponential factors were calculated from the resulting slopes and intercepts. Table 2 summarizes these results. The temperature dependence of the rate constants is shown below.

$$k'_{A1}((\mathrm{L}^2\,\mathrm{mol}^{-2})/\mathrm{min}) = (1.99 \times 10^5) \exp\left(\frac{-16.5\ (\mathrm{kcal/mol})}{T}\right) \tag{20}$$

$$ {}^2k_{B1}((\mathrm{L}\,\mathrm{mol}^{-1})/\mathrm{min}) = (1.13 \times 10^5) \exp\left(\frac{-16.76\ (\mathrm{kcal/mol})}{T}\right) \tag{21}$$

$$k'_{A2}((\mathrm{L}^2\,\mathrm{mol}^{-2})/\mathrm{min}) = (4.05 \times 10^4) \exp\left(\frac{-13.1\ (\mathrm{kcal/mol})}{T}\right) \tag{22}$$

Several characteristics of the reaction mechanism proposed herein should be considered at this point. Obviously, direct spectroscopic observation of the proposed intermediates would be desirable; in fact, such data would permit unambiguous identification of the reaction mechanism. However, distinguishing between the proposed hydrogen-bonded species would be difficult based upon the NIR data obtained to date.

While direct spectroscopic identification would be ideal, the mathematical model proposed is valid throughout the course of the reaction, even during the initial and final stages. The model describes the data well on the basis of only two rate constants. The order of the reaction was not an adjustable parameter; it was determined by the mechanism proposed. Finally, autocatalytic behavior and the resulting rate equations were not assumed initially; autocatalytic characteristics were a consequence of the details of the mechanism.

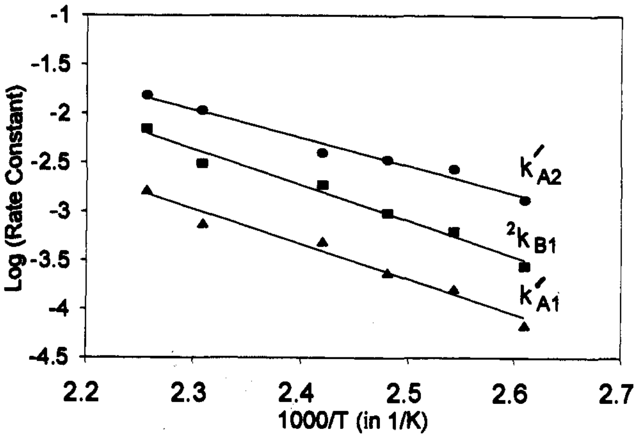

Figure 7. Arrhenius relations for rate constants k'_{A1}, ${}^2k_{B1}$, and k'_{A2}.

Table 2. Reaction Rate Constants Obtained by Least-Squares Regression Analysis

	383 K	393 K	403 K	413 K	423 K	433 K	E^c
$k'_{A1} \times 10^4$ [a]	0.687	1.63	2.41	5.00	7.59	16.58	16.5 ± 1.4
${}^2k_{B1} \times 10^6$ [b]	2.79	6.3	9.73	18.96	31.21	69.93	16.8 ± 1.2
$k'_{A2} \times 10^4$ [a]	13.34	27.27	33.71	39.72	107.71	153.58	13.1 ± 1.0

[a] In units of $(\mathrm{L}^2\,\mathrm{mol}^{-2})/\mathrm{min}$. [b] In units of (L mol)/min. [c] In units of kcal/mol with 95% confidence intervals.

Conclusions

In situ NIR spectroscopy has been shown to be an excellent tool for quantifying the progress of the epoxy–amine cure reactions. The changes in concentrations of epoxide, amine, and hydroxyl groups with time were followed unambiguously in the near-infrared region with high accuracy. Among previous proposed mechanisms for the epoxy amine cure reactions, some lacked theoretical justifications and thus were not considered. The experimental data fit with high accuracy a mechanistic model that includes one non-catalytic reaction path (A1 or B1) and one catalytic reaction path (A2). Each path contains three steps: (1) the formation of hydrogen-bonded epoxides or amines, (2) the formation of termolecular intermediates involving epoxides, amines, and hydroxyls, and (3) the decomposition of such intermediates through epoxide ring cleavage. The formation of termolecular intermediates has been shown to be the rate-determining step. The reaction rate constants obtained over a temperature range from 383 to 443 K demonstrated an Arrhenius temperature dependence and the corresponding activation energies and pre-exponential factors have been determined. The reaction rate constants for the catalytic reactions are significantly larger than those for the non-catalytic reactions. Therefore, epoxy resin cure rates are determined by the autocatalytic behavior of the system.

Acknowledgment. The authors gratefully acknowledge the financial support of the Engineering Experiment Station and the Advanced Manufacturing Institute at Kansas State University.